© 2020. Published by The Company of Biologists Ltd | Journal of Experimental Biology (2020) 223, jeb217687. doi:10.1242/jeb.217687

RESEARCH ARTICLE

Photoperiodic regulation in a wild-derived mouse strain

Cristina Sáenz de Miera[1,2,*,‡], Matthew Beymer[1], Kevin Routledge[2], Elżbieta Król[2], Colin Selman[2,3], David G. Hazlerigg[2,4] and Valérie Simonneaux[1]

ABSTRACT

MSM/Ms (MSM) is a mouse strain derived from Japanese wild mice, *Mus musculus molossinus*, that maintains the ability to synthesize melatonin in patterns reflecting the ambient photoperiod. The objective of this study was to characterize the effects of photoperiodic variation on metabolic and reproductive traits, and the related changes in pituitary–hypothalamic gene expression in MSM mice. MSM mice were kept in long (LP) or short photoperiod (SP) for 6 weeks. Our results demonstrate that MSM mice kept in LP, as compared with mice kept in SP, display higher expression of genes encoding thyrotropin (TSH) in the pars tuberalis, thyroid hormone deiodinase 2 (dio2) in the tanycytes and RFamide-related peptide (RFRP3) in the hypothalamus, and lower expression of dio3 in the tanycytes, along with larger body and reproductive organ mass. Additionally, to assess the effects of the gestational photoperiodic environment on the expression of these genes, we kept MSM mice in LP or SP from gestation and studied their offspring. We show that the gestational photoperiod affects the TSH/dio pathway in newborn MSM mice in a similar way to adults. This result indicates a transgenerational effect of photoperiod from the mother to the fetus *in utero*. Overall, these results indicate that photoperiod can influence neuroendocrine regulation in a melatonin-proficient mouse strain, in a manner similar to that documented in other seasonal rodent species. MSM mice may therefore become a useful model for research into the molecular basis of photoperiodic regulation of seasonal biology.

KEY WORDS: *Mus musculus molossinus*, Photoperiod, Melatonin, Reproduction, Pars tuberalis, TSH, Deiodinases, RFRP3

INTRODUCTION

Species living in temperate latitudes face challenging seasonal changes in the environment. The annual rhythm in photoperiod serves as a reliable signal to anticipate these changes and thus optimize transitions in physiology and behavior. In mammals, photoperiod perceived by the eyes is transduced by a complex neural pathway into the nocturnal production of melatonin by the pineal gland (Goldman, 2001). The neuroendocrine pathway decoding the melatonin photoperiodic message and its integration on the control of reproduction, metabolism or molt have been elucidated to a certain extent, using species which present robust seasonal changes in physiology, such as sheep or hamsters.

The pars tuberalis (PT) of the pituitary gland, which is melatonin-sensitive in mammals (Morgan et al., 1994; Weaver et al., 1989; Williams et al., 1989), is the critical neuroanatomical site where the photoperiodic melatonin signal is integrated. Exposure to short nocturnal melatonin profile under long days induces thyrotropin (TSH) expression in PT-specific thyrotrope cells, mainly via upregulation of *TSHβ* subunit expression, whereas exposure to long melatonin profile in short days downregulates TSH expression (Bockmann et al., 1996; Dardente et al., 2003; Wittkowski et al., 1988). PT TSH, in turn, acts on TSH receptor (TSHr)-expressing hypothalamic tanycytes, located on the wall of the third ventricle (3V) (Hanon et al., 2008; Klosen et al., 2013; Ono et al., 2008), where it upregulates type 2 (dio2) and downregulates type 3 (dio3) thyroid hormone deiodinase expression (Barrett et al., 2007; Revel et al., 2006b). dio2 transforms the circulating thyroxine (T4) form of TH into the active form triiodothyronine (T3), whereas dio3 degrades T3 and T4 to diiodothyronine and reverse T3, respectively. Thus, the opposite TSH-driven regulation in dio2/3 leads to higher intrahypothalamic levels of T3 in long (LP) as compared with short (SP) photoperiod. Central hypothalamic delivery of either TSH or T3 in SD-adapted hamsters and sheep restores summer physiology (Barrett et al., 2007; Hanon et al., 2008; Klosen et al., 2013; Murphy et al., 2012), demonstrating a role of the TSH/DIO/T3 neuroendocrine pathway in the photoperiodic control of seasonal metabolism and reproduction.

The photoperiodic TSH/T3 message has been proposed to control the hypothalamic reproductive network via the regulation of the neuropeptides RFamide related peptide 3 (RFRP3) in the dorsomedial ventromedial hypothalamus (DMH/VMH) and kisspeptin (Kp) in the arcuate nucleus (Arc) (Angelopoulou et al., 2019; Simonneaux, 2018). RFRP3 expression shows a conserved melatonin-driven inhibition leading to lower levels in SP as compared with LP in all species investigated (Ancel et al., 2012; Dardente et al., 2008; Janati et al., 2013; Revel et al., 2008; Sáenz de Miera et al., 2014; Smith et al., 2008; Ubuka et al., 2012), but its effect on reproductive activity shows species, sex and reproductive stage differences (Ancel et al., 2012; Henningsen et al., 2017; Ubuka et al., 2012). Kp is a well conserved activator of GnRH neurons, but Arc Kp expression is inhibited by both melatonin in SP and sex steroids in LP, leading to species-dependent differences in seasonal variation (Rasri-Klosen et al., 2017; Revel et al., 2006a; Sáenz de Miera et al., 2014; Smith et al., 2005). The mechanism through which RFRP3 and Kp neuronal activity are regulated by the photoperiodic changes in the TSH/T3 signal is currently unknown. Functional studies using genetic tools are required to fully unravel the molecular networks that integrate the photoperiodic signal into these neuroendocrine systems; such tools are scarce in 'traditional' photoperiodic models, but widely available in mice.

In contrast to seasonal rodent species, common laboratory mice strains present no signs of photoperiodic or seasonal transitions in metabolic and reproductive physiology, remaining reproductive all

[1]Institute for Cellular and Integrative Neuroscience, University of Strasbourg, 67000 Strasbourg, France. [2]School of Biological Sciences, University of Aberdeen, Aberdeen AB24 2TZ, UK. [3]Institute of Biodiversity, Animal Health and Comparative Medicine, University of Glasgow, Glasgow G12 8QQ, UK. [4]Department of Arctic and Marine Biology, Faculty of Biosciences, Fisheries and Economy, University of Tromsø, 9037 Tromsø, Norway.
*Present address: Department of Molecular and Integrative Physiology, The University of Michigan, Ann Arbor, MI 48109, USA.

‡Author for correspondence (csaenzde@umich.edu)

C.S.M., 0000-0001-8047-035X; M.B., 0000-0002-8070-3456; K.R., 0000-0001-5149-503X; C.S., 0000-0002-8727-0593; D.G.H., 0000-0003-4884-8409; V.S., 0000-0002-6004-7850

Received 31 October 2019; Accepted 10 February 2020

Journal of Experimental Biology (2020) 223, jeb217687. doi:10.1242/jeb.217687

List of abbreviations

Arc	arcuate nucleus
dio2	thyroid hormone deiodinase 2
dio3	thyroid hormone deiodinase 3
DMH/VMH	dorsomedial/ventromedial hypothalamus
Kp	Kisspeptin
LP	long photoperiod
PT	pars tuberalis
RFRP3	RFamide related peptide 3
SP	short photoperiod
T3	triiodothyronine
T4	thyroxine
TSH	thyrotropin
ZT	zeitgeber time

year round (Bronson, 1979; Laurie, 1946). However, studies using melatonin-deficient and -proficient mice have contributed to the functional characterization of the photoperiodic neuroendocrine pathway in mammals. Photoperiodic differences in *TSH*, *dio2* and *dio3* gene expression were observed in the melatonin-proficient CBA strain, while these photoperiodic differences were not observed in the melatonin deficient C57BL/6J (C57) strain, except when the latter received long-term melatonin administration (Ono et al., 2008). This study demonstrates that the TSH/dio2/3 pathway is conserved in mice, whether producing melatonin or not, although neither of these mice strains show photoperiodic differences in reproductive parameters (Ono et al., 2008).

MSM/Ms (MSM) is an inbred mouse strain derived from Japanese wild mice, *Mus musculus molossinus* Temminck 1844, captured in Japan in the 1970s (Goto et al., 1989); these mice maintain the ability to synthetize melatonin (Goto et al., 1989) with longer nighttime melatonin production in SP than in LP (Kasahara et al., 2010). Notably, offspring of C57×MSM backcrosses show a moderate reduction in testis development associated with melatonin productivity (i.e. associated with carrying MSM allelic variants for melatonin synthesis enzyme genes) (Kasahara et al., 2010), suggesting a potential photoperiodic modulation of the central control of reproduction and metabolism in this strain.

The objective of the present study was to explore the effects of different photoperiodic exposure on pituitary–hypothalamic gene expression, reproductive neuropeptides and on physiology in the *M. musculus* strain MSM. Furthermore, as maternal melatonin impacts the metabolic and reproductive offspring development in the hamster (Sáenz de Miera et al., 2017; Weaver and Reppert, 1986), we also explored whether the gestational photoperiodic environment influences gene expression in newborn MSM offspring.

MATERIALS AND METHODS

Animals

Two different mouse strains were used: C57BL/6J (C57; purchased from Jackson, Bar Harbor, ME, USA) and *Mus musculus molossinus* (MSM; bred in-house from couples purchased from Jackson, with initial founders from the National Institute of Genetics, Mishima, Japan). Mice were maintained at the Chronobiotron (CNRS-UMS 3415) at the University of Strasbourg (photoperiodic and melatonin sampling experiment) and at the animal facilities in the Zoology building at the University of Aberdeen (gestational experiment). Upon arrival, in both animal facilities, mice were placed 3–5 per cage at a constant temperature (21±2°C) and humidity (55±5%), with food and water provided *ad libitum*, and under long photoperiod (LP: 16 h:8 h light:dark) with lights on at zeitgeber time 0 (ZT0). As indicated below, in some experimental paradigms, mice were transferred into short photoperiod (SP: 8 h:16 h light:dark) conditions.

Protocols were submitted to the Comité Régional d'Ethique en Matière d'Expérimentation Animale of the University of Strasbourg and to the Animal Welfare and Ethics Review Board at the University of Aberdeen. All experiments were conducted in accordance with the UK Home Office (Project Licence 60/4504) and the European Directive UE/63/2010 on the protection of animals used for scientific purposes.

Experimental design and tissue collection

A first cohort of C57 and MSM male mice was used to analyze the effect of photoperiod on reproductive physiology and neuroendocrine gene expression. Six-week-old individuals housed in LP were either kept under LP or transferred to SP conditions for approximately 6 weeks (N=22). At the end of the experiment, animals were euthanized by CO_2 inhalation and their body mass, seminal vesicle mass and paired testes mass were measured, and trunk blood was taken for hormone assays. Gonadosomatic index (GSI) was calculated as testis mass (mg)/body mass (g)×10. Animals were then transcardially perfused with periodate–lysine–paraformaldehyde (PFA) fixative. Brains were sampled and dehydrated through an ethanol gradient and embedded in polyethylene glycol, as previously described (Klosen et al., 1993).

As results of the first cohort indicated a robust photoperiodic integration, a second cohort of MSM mice was used to determine the photoperiodic change in the daily profile of melatonin. Adult male mice (3 to 7 months) were either kept under LP or transferred to SP conditions for 6 weeks, then euthanized by CO_2 inhalation at different times of the day (ZT2, ZT8, ZT17, ZT19, ZT21 and ZT23 under LP; ZT4, ZT9, ZT12, ZT16, ZT20 and ZT23 under SP, N=53). Pineal glands were sampled and stored at −20°C for further melatonin assay.

A third cohort of MSM was used to study the effects of photoperiodic exposure *in utero*. Two-month-old male and female MSM mice were paired in LP, and 3 days after pairing, all males were removed from the cages, and half of the females were maintained under LP while the other half was transferred to SP. All female mice were checked daily for births, and the day a litter was found was assigned as P0 for that litter. At each sampling point, whole litters were culled and each group included animals from at least three different litters. The first sampling was done at P1; at this point, whole litters – including the dams – were culled for the study. Offspring from the remaining litters were kept in the same gestational photoperiod, were weaned at 3 weeks of age and siblings were placed in same-sex cages. At the second sampling point, at P50, whole cages of animals from LP or SP were culled for the study (N=47). At culling, newborns were decapitated and the full head was snap-frozen and stored at −80°C until processed for gene expression analysis. P50 and dams were killed by cervical dislocation, the body and sex organs (testis in males and both ovaries and uterine horns in females) were weighed, and brains were dissected, snap-frozen and stored at −80°C until processed for gene expression analysis.

Detection of mRNA by *in situ* hybridization

Gene expression was analyzed by non-radioactive *in situ* hybridization in the first cohort of C57 and MSM male mice under LP or SP and by radioactive *in situ* hybridization in the third cohort of MSM mice under gestational LP or SP.

Non-radioactive *in situ* hybridization was performed with 300 to 400 bp antisense riboprobes selective for the mouse *TSHβ*

(NM_009432.2), *dio2* (NM_010050.4), *dio3* (NM_172119.2) and *rfrp* (NM_021892.1) and rat *kiss1* (NM_181692.1) genes, labeled with digoxigenin (DIG RNA labeling kit, Roche, Meylan, France) and hybridized on 10 µm-thick coronal brain sections as already described (Klosen et al., 2013). Briefly, sections (one in 10 throughout the hypothalamus), mounted on SuperFrost ultraplus slides (Menzel-Glaser, Brunswick, Germany), were postfixed in PFA 4% in phosphate buffer (PB) for 10 min at room temperature, rinsed with PBS, treated with 0.5 µg ml^{-1} proteinase K (Roche) for 30 min at 37°C, rinsed with ice-cold PFA 2% in PB, rinsed again in PBS, acetylated twice for 10 min with 0.25% acetic anhydride in 100 mmol l^{-1} triethanolamine (TEA) and finally equilibrated in 5× saline-sodium citrate (SSC) 0.05% tween 20% (TW20) twice for 5 min at room temperature. Hybridization was performed with 2 µg ml^{-1} antisense probe in a medium containing 50% formamide, 5× SSC, 5× Denhardt's solution, 0.1% TW20 and 1 mg ml^{-1} salmon sperm DNA for 40 h at 60°C. High-stringency washes were performed with 0.1× SSC 0.05% TW20 at 72°C to reduce nonspecific labeling. The DIG tag was detected using an alkaline phosphatase-coupled anti-digoxigenin antibody (1:5000, Roche). Alkaline phosphatase activity was visualized with a mixture of Nitro Blue Tetrazolium/Bromo-Chloro-Indolyl Phosphate for 1 to 2 h and stopped before the staining intensity reached saturation. After detection, slides were premounted using Crystalmount aqueous mounting medium (Sigma-Aldrich, Saint-Quentin-Fallavier, France) and mounted with Eukitt® (Sigma-Aldrich).

For the radioactive *in situ* hybridization, antisense rat *TSHβ* (GenBank accession number M10902) and vole *dio2* and *dio3* (Król et al., 2012) riboprobes were labeled with ^{35}S-UTP, followed by column purification (Illustra probe quant G-50 micro-columns; GE Healthcare, Little Chalfont, UK) and hybridization was performed as already described (Król et al., 2012). Briefly, 16 µm-thick coronal sections, one in eight sections throughout the hypothalamus, were mounted on poly-L-lysine coated slides, fixed in ice-cold 4% PFA, dehydrated in serial alcohol baths and acetylated in 0.25% acetic anhydride in 0.1 mol l^{-1} TEA. Sections were hybridized overnight at 60°C using approximately 5×10^5 cpm labeled probe per slide determined by liquid scintillation counting. The next day, slides were subjected to digestion with RNAse-A for 30 min at 37°C and high-stringency washes with 2×, 1×, 0.5× SSC for 10 min at room temperature and 0.1× SSC at 60°C for 30 min to remove non-specific probe binding. Finally, slides were dehydrated in serial alcohols and exposed to film autoradiography (Kodak, Rochester, NY, USA), with exposure for 2–4 weeks according to intensity of the hybridization signal.

Image analysis

Brain sections of all animals of a given experiment were treated and analyzed similarly together, to ensure identical conditions, and a person blind to the animal's experimental setup quantified the *in situ* hybridization signals.

For the non-radioactive *in situ* hybridization, photos were taken at 10× magnification using a Leica DMRB microscope (Leica Microsystems, Rueil-Malmaison, France) with an Olympus DP50 digital camera (Olympus France, Rungis, France), and digital images were captured using the camera software ViewfinderLite (Olympus), ensuring that all lighting parameters were consistent for all images. A background image was taken for each slide and subtracted from the labeling measure. All measurements were taken using ImageJ software (National Institutes of Health, Bethesda, MD, USA) according to an earlier published protocol (Sáenz de Miera et al., 2017). *TSHβ* and *dio2* quantification was made using the 'segmented line' tool to cover the staining of *TSHβ* all along the PT and *dio2* in the tanycyte cell bodies, on the paraventricular zone (PVZ). Three consecutive sections along the rostro-caudal axis were measured per animal. The mean gray value in arbitrary units for each animal was calculated as the average of the three measurements. *kiss1* mRNA was quantified as the mean pixel gray level of staining in 'elliptical' sections of the same area for each neuronal cell body. A minimum of 20 neuronal cell bodies were quantified per animal in sections corresponding to the level of the mid ARC region. For *rfrp* mRNA, the total number of labeled neurons was hand-counted on the Leica DMRB microscope in all sections to cover the rostro-caudal hypothalamic expression of *rfrp* and given as number of positive neurons per animal.

For radioactive *in situ* hybridization, autoradiography films were scanned with an Epson 1640XL transmittance scanner at 720 dpi along with a calibrated series of optical density (OD) standards. OD measurements were analyzed for all genes using ImageJ software. The mean OD signal measured on all brain sections for a given gene is the OD value reported for each animal.

Hormone assays

Testosterone levels were measure by ELISA using the Parameter Testosterone Assay (R&D Systems, Minneapolis, MN, USA), with a sensitivity of 0.041 ng ml^{-1}. FSH levels were measured by radioimmunoassay (RIA) by Dr Manuel Tena-Sempere (University of Córdoba, Spain) as previously described (García-Galiano et al., 2012). Melatonin levels were measured in individual pineal glands by RIA (Ribelayga et al., 1999).

Statistical analysis

All data are represented as means±s.e.m. of *n* animals per experimental group. Sample sizes in the study were based on our previous work looking at similar response variables in other seasonal rodents (Król et al., 2012; Sáenz de Miera et al., 2014, 2017), typically allowing us to resolve differences of 20% or more between means as statistically significant. All data were checked for normality using the Shapiro–Wilk test and homogeneity of variance using the *F*-test. When data were not normally distributed, they were transformed to fit this distribution and reanalyzed. Data were analyzed for photoperiodic differences by the two-tailed *t*-test, or Mann–Whitney test when data were not normally distributed. Two-way ANOVA analysis with photoperiod and sex as factors was used to analyze the photoperiodic differences in GSI and to assess a possible effect of sex on gene expression in P50 offspring. Pearson correlation analysis was used to evaluate the correlation between different genes. All statistical analyses were performed using PRISM, version 7 (GraphPad Software Inc., San Diego, CA, USA).

RESULTS

Effect of photoperiod on adult MSM mice

To analyze the effect of photoperiod on reproductive physiology and neuroendocrine gene expression, we kept adult male C57 and MSM mice in LP or transferred them to SP for 6 weeks prior to euthanization.

In adult MSM, we collected pineal glands to explore how melatonin production is affected by photoperiod. Pineal melatonin content was low during the light period and increased during the dark period in both photoperiodic states (Fig. 1A). In LP, a modest increase in average melatonin content was observed at ZT21, but no significant regression of the melatonin peak was observed (r^2=0.86, P=0.20); therefore, peak duration could not be calculated. In SP, the

Journal of Experimental Biology (2020) 223, jeb217687. doi:10.1242/jeb.217687

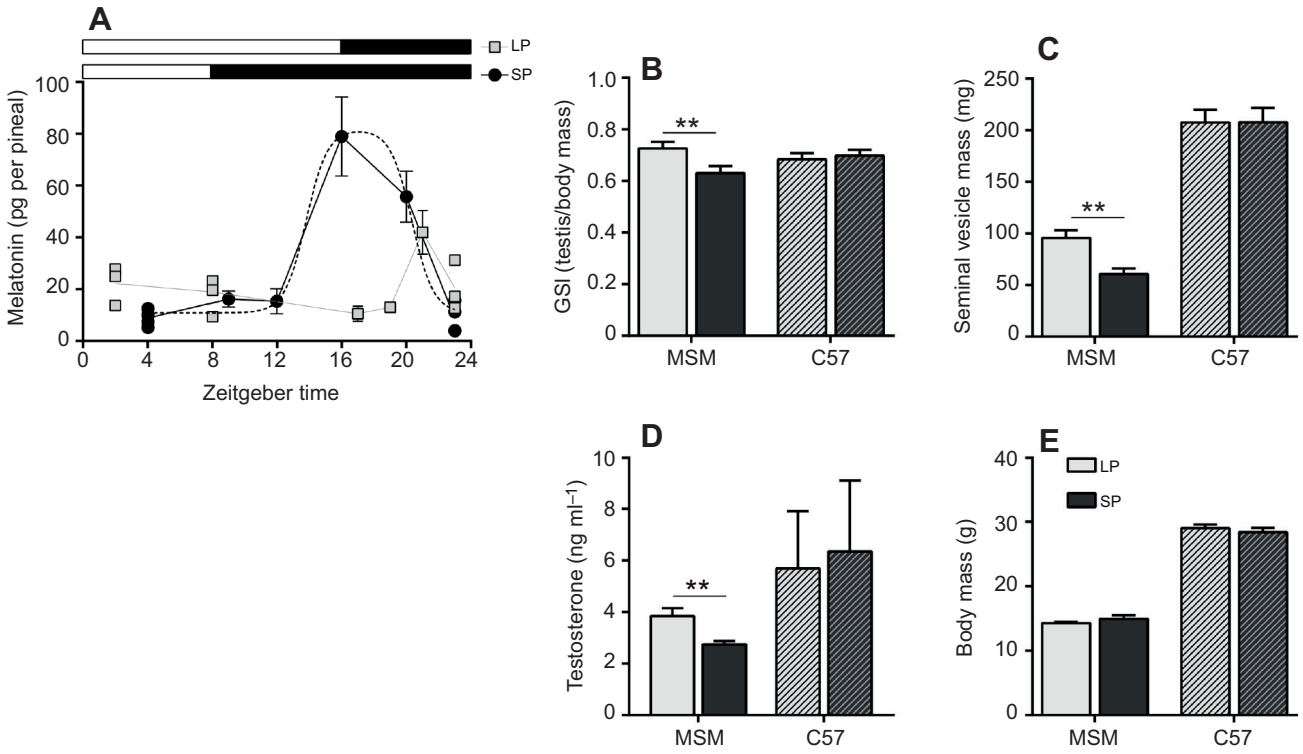

Fig. 1. Effects of photoperiodic exposure in melatonin profile and physiology in adult mice. (A) Pineal melatonin content (pg per pineal gland) at different times of the day assayed by radioimmunoassay in adult male MSM mice kept in long (LP) or short (SP) photoperiod for 6 weeks. A significant rhythm was observed in SP-exposed mice (nonlinear regression: r^2=0.99, P=0.015; n=28 in SP, n=25 in LP). Data are means±s.e.m. of n=3–6 individual pineal glands per photoperiod and time point. Zeitgeber time 0=lights on time. White and black bars designate the light and dark phase, respectively. (B) Gonadosomatic index (GSI: testis mass/body mass), (C) seminal vesicle mass (mg), (D) blood testosterone levels (ng ml^{-1}) and (E) body mass (g) of individual adult male MSM and C57 mice kept in LP or SP for 6 weeks (N=21; n=5 MSM in LP, n=5 MSM in SP, n=6 C57 in LP, n=5 C57 in SP). Data are means±s.e.m. **P<0.01 for LP versus SP by two-tailed t-test.

averaged melatonin concentration showed a maximum concentration 6 h after lights off. The result of nonlinear regression analysis indicated a significant melatonin rhythm in SP (r^2=0.99, P=0.015) of 6.56 h long with a peak onset estimate (φ_1) at ZT13.8 and an offset estimate (φ_2) at ZT20.4. The maximal mean nocturnal melatonin level measured was higher in SP (y_{max}=78.98±34.15 ng ml^{-1}) as compared with LP (y_{max}=41.99±20.74 ng ml^{-1}).

In adult male MSM, all of the reproductive parameters varied significantly between photoperiods (Fig. 1B–D), with significantly smaller testis mass (P<0.05, t-test; not shown), testis/body mass ratio (P<0.01, t-test; Fig. 1B), seminal vesicle mass (P<0.01, t-test; Fig. 1C) and testosterone concentration (P<0.01, t-test; Fig. 1D) in SP than in LP. Circulating FSH tended to exhibit lower levels in SP MSM mice as compared with LP (17.17±1.98 ng ml^{-1} in LP versus 12.51±1.68 ng ml^{-1} in SP; P=0.11, data not shown). Body mass remained unchanged between LP- and SP-exposed MSM mice (P=0.24, t-test; Fig. 1E). In C57 mice, all the physiological parameters measured showed no photoperiodic variations (LP versus SP, P>0.05; t-tests; Fig. 1B–E).

In MSM mice transferred from LP to SP, PT *TSHβ* expression (P<0.01, Mann–Whitney test; Fig. 2A) and tanycytic *dio2* expression (P<0.001; t-test; Fig. 2B) significantly decreased by 5- and 3-fold, respectively. Furthermore, *TSHβ* and *dio2* mRNA levels were strongly correlated in MSM mice (Pearson r=0.82, P<0.01). *dio3* expression was hardly detectable in LP-exposed animals, but showed a large increase in SP-exposed animals (P<0.01, t-test; Fig. 2D). The number of *rfrp*-expressing neurons was markedly reduced after transfer from LP to SP (P<0.001, t-test; Fig. 2E), but *kiss1* expression was not significantly different between LP and SP, albeit a tendency to be lower in SP (P=0.07, t-test; Fig. 2F). In C57 mice, transfer from LP to SP did not affect any of these investigated genes (Fig. 2).

Notably, in MSM mice only, strong correlations were observed between *dio2* mRNA levels and the number of *rfrp*-expressing cells (MSM: Pearson r=0.93, P<0.001; C57: Pearson r=−0.16, P=0.64; Fig. 2G), as well as between the number of *rfrp*-expressing neurons and testicular size (MSM: Pearson r=−0.77, P<0.01; C57: Pearson r=−0.39, P=0.24; Fig. 2H).

Effects of gestational photoperiod on MSM physiology and neuroendocrine gene expression

To explore the effects of photoperiodic exposure *in utero*, pregnant MSM females were either maintained in LP or transferred to SP, and pups were further maintained in the gestational photoperiod until P50. At P50, female and male offspring gestated and raised in LP showed approximately 1.2-fold larger body mass than those kept in SP (P<0.001 for females, Mann–Whitney test; P<0.0001 for males, t-test; Fig. 3A). Reproductive organ mass was also larger in LP- as compared with SP-treated mice, in females showing 3-fold heavier reproductive organs, and in males showing 1.3-fold heavier testis mass in LP as compared with SP (P<0.0001 for uterus mass, P<0.001 for testis mass, t-tests; Fig. 3B). As a result, GSI analysis showed that the effect of SP exposure was more profound in females than in males (P<0.05 for interaction between sex and photoperiod, two-way ANOVA). In LP females, GSI was 2.5-fold larger than in SP females (P<0.001; *post hoc* Tukey test; Fig. 3C), whereas it was similar in males in both photoperiods (P=0.83, *post hoc* Tukey test).

Journal of Experimental Biology (2020) 223, jeb217687. doi:10.1242/jeb.217687

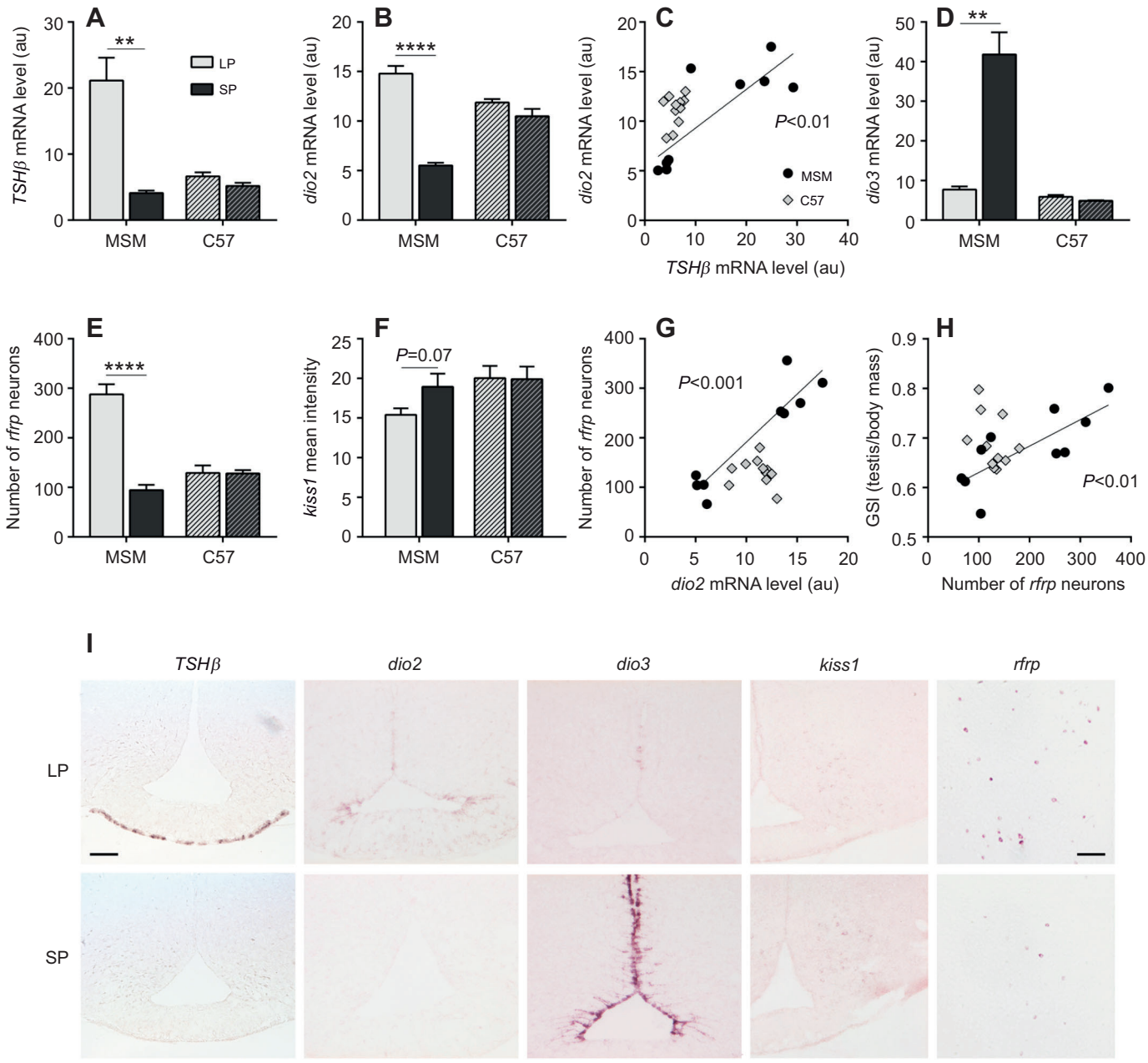

Fig. 2. Effects of photoperiodic exposure on pituitary and hypothalamic gene expression in adult mice. (A,B,D) Photoperiodic variation in *TSHβ* expression in the pars tuberalis (PT) and *dio2* and *dio3* expression in the hypothalamus in MSM and C57 adult male mice in LP or SP conditions. (C) Scatterplot showing the positive correlation between *TSHβ* expression in the PT and *dio2* expression in the hypothalamus in MSM mice (r=0.82, r^2=0.67; P<0.01) and lack of correlation in C57 mice (r=0.38, r^2=0.14, P=0.25). (E,F) Photoperiodic variation in the number of *rfrp*-expressing neurons in the DMH/VMH and in *kiss1* cell mean intensity in the arcuate nucleus (Arc) in MSM and C57 adult male mice in LP and SP conditions. (G) Scatterplot showing the positive correlation between *dio2* expression in the hypothalamus and the number of *rfrp* neurons in the dorsomedial/ventromedial hypothalamus (DMH/VMH) in MSM mice (r=0.93, r^2=0.86, P<0.001) and lack of correlation in C57 mice (r=−0.16, r^2=0.02, P=0.64). (H) Scatterplot showing the positive correlation between the number of *rfrp* neurons in the DMH/VMH and the GSI in MSM mice (r=0.77, r^2=0.59, P<0.01) and lack of correlation in C57 mice (r=−0.39, r^2=0.15, P=0.24; N=22; n=5 MSM in LP; n=5 MSM in SP; n=6 C57 in LP; n=6 C57 in SP). Data are means±s.e.m. **P<0.01 and ****P<0.0001 for LP versus SP by two-tailed t-test. (I) Representative images of *TSHβ* labeling in the PT, *dio2* and *dio3* labeling in the paraventricular zone of the hypothalamus, *kiss1* labeling in the Arc and *rfrp* labeling in the DMH/VMH region of the hypothalamus determined by non-radioactive *in situ* hybridization in adult male MSM mice in LP and SP conditions. Scale bars=100 µm for *TSHβ*, *dio2*, *dio3* and *kiss1* images and 50 µm for *rfrp* images.

Although GSI was similar for males and females in LP (P=0.48, *post hoc* Tukey test), it was 2.6-fold smaller in females as compared with males in SP. Therefore, somatic and reproductive growth is affected by different photoperiodic exposure from gestation in MSM animals in both sexes, although there is a more profound effect on female reproductive organs.

In P50 offspring, no sex differences were found in any of the genes studied at the same photoperiodic state (not shown, two-way ANOVA, factor sex: *TSHβ*: P=0.13; *dio2*: P=0.41; *dio3*: P=0.77; *rfrp*: P=0.08); therefore, data from male and female offspring were combined to increase the power for the photoperiodic analysis (N=14). *TSHβ* gene expression in the PT was significantly higher in

Journal of Experimental Biology (2020) 223, jeb217687. doi:10.1242/jeb.217687

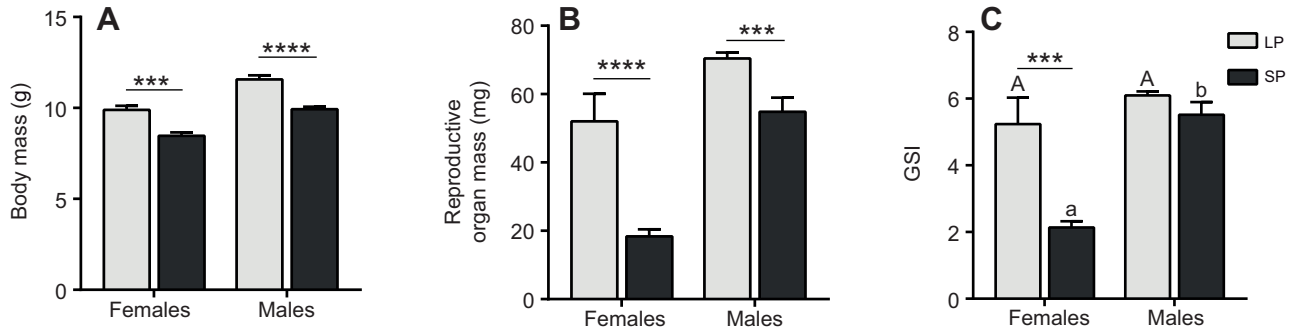

Fig. 3. Effects of photoperiodic exposure from gestation on physiology in adult female and male MSM offspring. (A) Body mass (g), (B) reproductive organ mass (mg) and (C) GSI (reproductive organ/body mass) of P50 animals kept in LP or SP conditions from gestation. Whole cages were culled at each point. Each group contains data from four cages (N=47; n=13 females in LP; n=9 females in SP; n=17 males in LP; n=8 males in SP). Data are means±s.e.m. ***P<0.001, ****P<0.0001 for LP versus SP by two-tailed t-test or main effects of two-way ANOVA (GSI). Different letters indicate differences between groups by Tukey *post hoc* analysis. Uppercase letters are used to compare females and males in LP. Lowercase letters are used to compare females and males in SP.

newborns and P50 offspring, and was higher also in dams exposed to LP as compared with SP (P<0.0001 for P1; P<0.001 for P50; t-tests; Fig. 4A,D). *dio2* gene expression in the PVZ of the 3V and the median eminence was significantly higher in LP than in SP at P50 and P1, and was also higher in LP- than in SP-exposed dams (P<0.01 for P1; P<0.001 for P50; t-tests; Fig. 4B,D). *dio3* gene expression in the PVZ was higher in dams exposed to SP and barely detectable in those exposed to LP during pregnancy. In contrast, *dio3* gene expression was detected at very low levels with no significant photoperiodic differences at P1 (P=0.12, t-test), and was significantly higher in SP at P50 (P<0.05, Mann–Whitney test; Fig. 4C,D). Hence, *TSHβ* and *dio2* expression reflected the photoperiod to which the mice were exposed in all groups, with a strong positive correlation observed between the levels of *dio2* and *TSHβ* expression in all dams and P50 animals combined (Pearson r=0.75, P<0.001) and at P1 (Pearson r=0.67, P<0.01; Fig. 4E).

The number of *rfrp*-expressing neurons tended to decrease in dams transferred to SP as compared with those maintained in LP during pregnancy (Fig. 4F). At P50, animals gestated and raised in LP had more than two times more *rfrp*-expressing neurons than those raised in SP (P<0.0001, t-test; Fig. 4F). At this age, *dio2* mRNA levels and the number of *rfrp*-expressing cells showed a positive correlation (Pearson r=0.75, P<0.01; Fig. 4G).

DISCUSSION

Seasonal rodents, in contrast to most mouse strains, show robust photoperiodic changes in gene expression in the neuroendocrine network comprising PT TSH and hypothalamic deiodinases, which in turn modulate the central regulation of the reproductive and metabolic axes. In the present study, we show that MSM mice exhibit photoperiodic regulation of reproductive organ and body mass, and testosterone levels in males, associated with corresponding changes in the TSH/dio network as well as RFRP expression. Furthermore, when exposure to different photoperiods in males and females starts from gestation, the reproductive and mass effects on offspring are more pronounced. These are the first results in *M. musculus* to show an integration of the photoperiodic signal on reproductive neuropeptides and gonadal development. Overall, the photoperiodic response observed in MSM mice appears comparable, albeit of lesser magnitude, to that in classical long-day breeders such as hamsters.

A 6 week exposure of male MSM mice to SP was sufficient to reduce testis size by approximately 15%, as well as reduce circulating testosterone and seminal vesicle mass, as compared with mice maintained in LP, indicating that MSM mice integrate photoperiod into the reproductive axis. Indeed, MSM mice exposed to SP showed a large nocturnal peak in pineal melatonin content that was markedly reduced under LP exposure, as previously observed in plasma (Kasahara et al., 2010). The large SP-induced melatonin production was accompanied by a robust decrease in PT *TSHβ* and tanycytic *dio2* expression and an increase in tanycytic *dio3* expression, consistent with the conserved photoperiodic response of these genes in vertebrates (Nakane and Yoshimura, 2014). These results are in agreement with those obtained in other melatonin-proficient mouse strains such as CBA or C3H, which display similar photoperiodic changes in melatonin rhythms (von Gall et al., 2000) mediating changes in expression of PT *TSHβ* and *dio2*/*3* in hypothalamic tanycytes (Ono et al., 2008; Yasuo et al., 2009). Despite the different melatonin profiles in MSM mice, we have not verified whether the changes observed in physiology and gene expression in this study are indeed mediated by melatonin, as confirmed in other photoperiodic mammals. As previously observed, C57 mice that lack a melatonin rhythm and show overall low levels of melatonin production (Ebihara et al., 1986; Vivien-Roels et al., 1998) displayed no photoperiodic changes in *TSHβ* and *dio2*/*3*. However, C57 mice remain responsive to melatonin administration with similar changes in TSH and deiodinase genes (Ono et al., 2008).

Both DMH/VMH RFRP3 and ARC Kp neurons have been proposed to take part in the photoperiodic control of reproduction (Ancel et al., 2012; Caraty et al., 2007; Klosen et al., 2013; Rasri-Klosen et al., 2017; Revel et al., 2006a, 2008; Ubuka et al., 2012). Here, we observed that the number of *rfrp*-expressing neurons was markedly higher in LP- as compared with SP-exposed MSM mice, but not in C57 mice. In addition, photoperiodic changes in *dio2* and *rfrp* expression were strongly correlated. Based on what has been consistently observed in other seasonal species (Klosen et al., 2013; Lomet et al., 2018; Revel et al., 2006b, 2008; Sáenz de Miera et al., 2014; Ubuka et al., 2012), this result suggests that the photoperiodic signal is transmitted to RFRP-expressing neurons via the melatonin-regulated TSH/dio network also in MSM mice. Interestingly, the level of *rfrp* expression was also correlated to testicular size in adult male MSM mice, further suggesting a regulatory role of RFRP3 in the photoperiodic changes in gonadal growth. Although photoperiodic changes in RFRP3 expression are highly conserved, the functional role of RFRP3 in seasonal reproduction is still discussed (Angelopoulou et al., 2019). In SP-adapted male Syrian (Ancel et al., 2012) and Siberian hamsters (Ubuka et al.,

Journal of Experimental Biology (2020) 223, jeb217687. doi:10.1242/jeb.217687

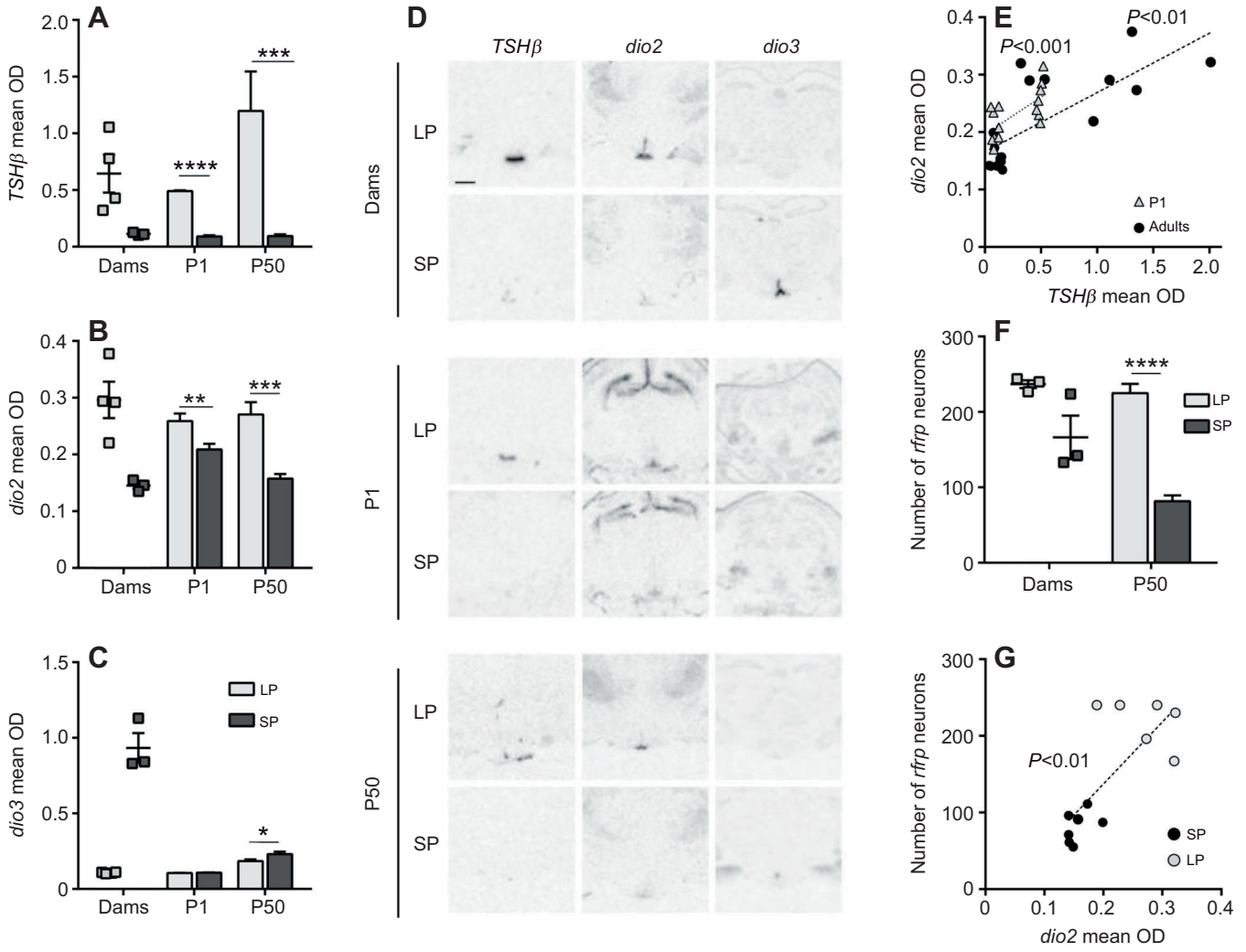

Fig. 4. Effects of photoperiodic exposure from gestation on pituitary and hypothalamic gene expression in MSM mice during development. (A–C) Mean *TSHβ* optic density (OD) in the PT and *dio2* and *dio3* OD in the hypothalamus at birth in dams and newborns (P1), and in adult offspring exposed to LP or SP conditions from gestation. (D) Representative autoradiographs of *TSHβ*, *dio2* and *dio3* gene expression determined by radioactive *in situ* hybridization in dams, P1 and P50 MSM mice exposed to LP or SP from gestation. Scale bar=1 mm. (E) Scatterplot showing the positive correlation between *TSHβ* expression in the PT and *dio2* expression in the hypothalamus in adult (dams and P50 combined) and newborn (P1) MSM mice (adults: r=0.75, r^2=0.57, P<0.001; newborns: r=0.67, r^2=0.45, P<0.01). (F) Photoperiodic variation in the number of *rfrp*-expressing neurons in the DMH/VMH determined by non-radioactive *in situ* hybridization in dams and in adult offspring exposed to long LP or SP from gestation. (G) Scatterplot showing the positive correlation between *dio2* expression in the hypothalamus and the number of *rfrp*-expressing neurons in the DMH/VMH in P50 MSM offspring (r=0.75; r^2=0.56; P<0.01). Whole litters were culled at each point. Each group contains data from 3–6 litters (n=4 dams in LP; n=3 dams in SP; n=7 P1 in LP; n=8 P1 in SP; n=7 P50 in LP; n=7 P50 in SP). Data are mean±s.e.m. **P<0.01, ***P<0.001, ****P<0.0001 for LP versus SP by two-tailed t-test.

2012) and in male mice (Ancel et al., 2017), central RFRP3 delivery has been shown to stimulate luteinizing hormone (LH) secretion. In female rodents, however, acute injection of RFRP3 inhibits the LH surge (Ancel et al., 2017; Henningsen et al., 2017), whereas chronic RFRP3 is able to restore ovarian activity in SP-adapted female Syrian hamsters (Henningsen et al., 2017). On the contrary, ARC *kiss1* expression was similar in both photoperiods in both MSM and C57 mice, despite a clear tendency to be lower in LP-kept MSM mice, probably reflecting the negative feedback effect of increased testosterone in these mice (Smith et al., 2005). Altogether, these data suggest that in male MSM mice, the TSH-driven photoperiodic change in dio2/3 regulates RFRP3 synthesis, which in turn may impact testicular activity. Further experiments are required to delineate whether the same regulation is observed in female MSM and whether RFRP3 is able to mediate the photoperiodic change in MSM reproduction.

Photoperiodic differences in maternal melatonin during gestation are known to impact the metabolic and reproductive development of Siberian hamster pups (Sáenz de Miera et al., 2017; Stetson et al., 1986). Here, we observed that when different photoperiodic exposure was applied on MSM mice from gestation to P50, male and female offspring exhibited a larger SP-induced reduction in reproductive organs, and a reduction in body mass, as compared with adult-only SP exposure. This suggests that maternal exposure to different photoperiods leads to a profound integration of the photoperiodic message into both the metabolic and the reproductive axes during development. Notably in females, prenatal SP exposure led to a reduction of approximately 60% in reproductive organ size as compared with prenatal LP exposure, possibly leading to an impairment of fertility. Maintenance of female C57 in SP from gestation has also been shown to delay the age of puberty through a decrease in body mass (Bohlen et al., 2018), highlighting that cues

alternative to melatonin-mediated photoperiodism may contribute to seasonality under some circumstances.

SP exposure during pregnancy led to a large reduction in *TSHβ* and *dio2* expression in dams and in newborns as compared with LP exposure, suggesting that the pups' photoperiodic system is responsive to maternal melatonin *in utero*, as we recently observed in Siberian hamsters (Sáenz de Miera et al., 2017). Further, the lower expression of these genes was maintained when the mice were kept in SP until P50. *dio3* expression was markedly increased in the dams exposed to SP only during gestation, i.e. for 20–21 days, remained low with no photoperiodic difference at birth, and was slightly higher in SP again at P50. This large increase under short, but not prolonged SP exposure, suggests a transitory *dio3* response to SP. The prediction is that *dio3* expression would increase through mid-lactation in SP maintained mice, as observed in hamsters (Sáenz de Miera et al., 2017). Such a transitory regulation of *dio3* expression is also observed in Siberian hamsters under decreasing natural photoperiod (Petri et al., 2016) or prolonged SP in laboratory settings (Milesi et al., 2017). These results suggest that the *dio3* effect in depleting hypothalamic T3 is only temporarily required for the 'winter' transition in physiology (Sáenz de Miera, 2019). Alternatively, *dio3* expression in MSM mice could be induced only after a transfer to a shorter photoperiod, and thus may not have happened in the mice born and raised in SP. These results do not allow us to distinguish between both possibilities, and further studies are required to discern the need of *dio3* expression (i.e. of T3 local depletion) in the transition to winter physiology.

In line with the inhibitory effect of SP exposure from pregnancy to P50 on *TSHβ* and *dio2* expression, the number of *rfrp*-expressing cells was more than two times lower in SP- as compared with LP-exposed mice. Interestingly, dams exposed to SP for only the duration of pregnancy showed a trend, but not a significant decrease in the number of *rfrp*-expressing neurons, confirming the slow dynamic of photoperiod-driven change in RFRP3 expression (Milesi et al., 2017; Revel et al., 2008).

Collectively, our results indicate that the TSHβ/DIOs/RFRP pathway is photoperiodically regulated in MSM mice, as observed in classical seasonal rodents. This regulation is associated with significant, albeit minor, changes in gonadal size, notably when the photoperiodic exposure starts *in utero*. Whether there is a photoperiodic change in hypothalamic T3, consequent to the dio2/dio3 switch, and whether this change by itself or through RFRP3 neurons is critical for the photoperiodic change in gonadal size observed in MSM mice remain to be established. The present results suggest that the ability to show photoperiodic responses in the reproductive axis is present in *M. musculus*. In most laboratory mouse strains, opportunistic strategies prevail, probably owing to artificial laboratory selection for breeding efficiency in animal facilities under a constant photoperiod or possibly reflecting their recent eco-evolutionary history as commensals to humans (Bronson, 1979).

The existence of a physiological endpoint reflecting the integration of the photoperiodic message highlights the value of these mice as models for genetic manipulations of this system. The use of genetic animal models has generated large advances in our knowledge of neuronal circuits, developmental processes and neuroendocrine integration (Elias, 2014). For the mammalian photoperiodic response, transgenic *TSHr* and *mt1r* knockout on a C57 background have served to establish the role of these receptors in the PT/MBH processing of the melatonin message (Ono et al., 2008; Yasuo et al., 2009). But owing to their lack of seasonal phenotype, genetic analysis of downstream neuroendocrine pathways and physiological consequences have been unexplored in these lines. Because crossing of transgenic lines onto an MSM background is readily feasible, it will now be possible to address this gap, and to take genetic approaches to analyze the downstream coupling of the PT/MBH axis.

Acknowledgements
The authors thank Béatrice Bothorel for her help on the melatonin regression analysis and Clarisse Quignon for her help with the microscope images. The authors thank the National Institute of Genetics, Japan, for providing the MSM mice used in this study.

Competing interests
The authors declare no competing or financial interests.

Author contributions
Conceptualization: C.S.M., C.S., D.G.H., V.S.; Methodology: C.S.M., M.B., D.G.H., V.S.; Formal analysis: C.S.M., M.B.; Investigation: C.S.M., M.B., K.R., E.K., D.G.H.; Resources: C.S.; Data curation: C.S.M.; Writing - original draft: C.S.M., V.S.; Writing - review & editing: C.S.M., M.B., K.R., E.K., C.S., D.G.H., V.S.; Visualization: C.S.M., V.S.; Supervision: D.G.H., V.S.; Funding acquisition: D.G.H., V.S.

Funding
This project was supported by a University of Strasbourg Institute for Advanced Studies fellowship [project: Epigenetic light] to D.G.H., and a grant from the Centre National de la Recherche Scientifique [Repramide ANR-13-BSV1-001] to V.S.

References
Ancel, C., Bentsen, A. H., Sébert, M.-E., Tena-Sempere, M., Mikkelsen, J. D. and Simonneaux, V. (2012). Stimulatory effect of RFRP-3 on the gonadotrophic axis in the male Syrian hamster: the exception proves the rule. *Endocrinology* **153**, 1352-1363. doi:10.1210/en.2011-1622

Ancel, C., Inglis, M. A. and Anderson, G. M. (2017). Central RFRP-3 stimulates LH secretion in male mice and has cycle stage-dependent inhibitory effects in females. *Endocrinology* **158**, 2873-2883. doi:10.1210/en.2016-1902

Angelopoulou, E., Quignon, C., Kriegsfeld, L. J. and Simonneaux, V. (2019). Functional implications of RFRP-3 in the central control of daily and seasonal rhythms in reproduction. *Front. Endocrinol.* **10**, 183. doi:10.3389/fendo.2019.00183

Barrett, P., Ebling, F. J. P., Schuhler, S., Wilson, D., Ross, A. W., Warner, A., Jethwa, P., Boelen, A., Visser, T. J., Ozanne, D. M. et al. (2007). Hypothalamic thyroid hormone catabolism acts as a gatekeeper for the seasonal control of body weight and reproduction. *Endocrinology* **148**, 3608-3617. doi:10.1210/en.2007-0316

Bockmann, J., Böckers, T. M., Vennemann, B., Niklowitz, P., Müller, J., Wittkowski, W., Sabel, B. and Kreutz, M. R. (1996). Short photoperiod-dependent down-regulation of Thyrotropin-alpha and -beta in hamster pars tuberalis-specific cells is prevented by pinealectomy. *Endocrinology* **137**, 1084-1813. doi:10.1210/endo.137.5.8612518

Bohlen, T. M., Silveira, M. A., Buonfiglio, D. D. C., Ferreira-Neto, H. C., Cipolla-Neto, J., Donato, J., , Jr and Frazao, R. (2018). A short-day photoperiod delays the timing of puberty in female mice via changes in the Kisspeptin system. *Front. Endocrinol.* **9**, 44. doi:10.3389/fendo.2018.00044

Bronson, F. H. (1979). The reproductive ecology of the house mouse. *Q. Rev. Biol.* **54**, 265-299. doi:10.1086/411295

Caraty, A., Smith, J. T., Lomet, D., Ben Saïd, S., Morrissey, A., Cognie, J., Doughton, B., Baril, G., Briant, C. and Clarke, I. J. (2007). Kisspeptin synchronizes preovulatory surges in cyclical ewes and causes ovulation in seasonally acyclic ewes. *Endocrinology* **148**, 5258-5267. doi:10.1210/en.2007-0554

Dardente, H., Klosen, P., Pévet, P. and Masson-Pévet, M. (2003). MT1 melatonin receptor mRNA expressing cells in the pars tuberalis of the European hamster: effect of photoperiod. *J. Neuroendocrinol.* **15**, 778-786. doi:10.1046/j.1365-2826.2003.01060.x

Dardente, H., Birnie, M., Lincoln, G. A. and Hazlerigg, D. G. (2008). RFamide-related peptide and its cognate receptor in the sheep: cDNA cloning, mRNA distribution in the hypothalamus and the effect of photoperiod. *J. Neuroendocrinol.* **20**, 1252-1259. doi:10.1111/j.1365-2826.2008.01784.x

Ebihara, S., Marks, T., Hudson, D. J. and Menaker, M. (1986). Genetic control of melatonin synthesis in the pineal gland of the mouse. *Science* **231**, 491-493. doi:10.1126/science.3941912

Elias, C. F. (2014). A critical view of the use of genetic tools to unveil neural circuits: the case of leptin action in reproduction. *Am. J. Physiol. Regul. Integr. Comp. Physiol.* **306**, R1-R9. doi:10.1152/ajpregu.00444.2013

García-Galiano, D., Pinilla, L. and Tena-Sempere, M. (2012). Sex steroids and the control of the Kiss1 system: developmental roles and major regulatory actions. *J. Neuroendocrinol.* **24**, 22-33. doi:10.1111/j.1365-2826.2011.02230.x

Goldman, B. D. (2001). Mammalian photoperiodic system: formal properties and neuroendocrine mechanisms of photoperiodic time measurement. *J. Biol. Rhythms* **16**, 283-301. doi:10.1177/074873001129001980

Goto, M., Oshima, I., Tomita, T. and Ebihara, S. (1989). Melatonin content of the pineal gland in different mouse strains. *J. Pineal Res.* **7**, 195-204. doi:10.1111/j.1600-079X.1989.tb00667.x

Hanon, E. A., Lincoln, G. A., Fustin, J.-M., Dardente, H., Masson-Pévet, M., Morgan, P. J. and Hazlerigg, D. G. (2008). Ancestral TSH mechanism signals summer in a photoperiodic mammal. *Curr. Biol.* **18**, 1147-1152. doi:10.1016/j.cub.2008.06.076

Henningsen, J. B., Ancel, C., Mikkelsen, J. D., Gauer, F. and Simonneaux, V. (2017). Roles of RFRP-3 in the daily and seasonal regulation of reproductive activity in female Syrian hamsters. *Endocrinology* **158**, 652-663. doi:10.1210/en.2016-1689

Janati, A., Talbi, R., Klosen, P., Mikkelsen, J. D., Magoul, R., Simonneaux, V. and El Ouezzani, S. (2013). Distribution and seasonal variation in hypothalamic RF-amide peptides in a semi-desert rodent, the jerboa. *J. Neuroendocrinol.* **25**, 402-411. doi:10.1111/jne.12015

Kasahara, T., Abe, K., Mekada, K., Yoshiki, A. and Kato, T. (2010). Genetic variation of melatonin productivity in laboratory mice under domestication. *Proc. Natl. Acad. Sci. USA* **107**, 6412-6417. doi:10.1073/pnas.0914399107

Klosen, P., Maessen, X. and van den Bosch de Aguilar, P. (1993). PEG embedding for immunocytochemistry: application to the analysis of immunoreactivity loss during histological processing. *J. Histochem. Cytochem.* **41**, 455-463. doi:10.1177/41.3.8429209

Klosen, P., Sébert, M.-E., Rasri, K., Laran-Chich, M.-P. and Simonneaux, V. (2013). TSH restores a summer phenotype in photoinhibited mammals via the RF-amides RFRP3 and kisspeptin. *FASEB J.* **27**, 2677-2686. doi:10.1096/fj.13-229559

Król, E., Douglas, A., Dardente, H., Birnie, M. J., van der Vinne, V., Eijer, W. G., Gerkema, M. P., Hazlerigg, D. G. and Hut, R. A. (2012). Strong pituitary and hypothalamic responses to photoperiod but not to 6-methoxy-2-benzoxazolinone in female common voles (*Microtus arvalis*). *Gen. Comp. Endocrinol.* **179**, 289-295. doi:10.1016/j.ygcen.2012.09.004

Laurie, E. M. O. (1946). The reproduction of the house-mouse (*Mus musculus*) living in different environments. *Proc. R. Soc. B Biol. Sci.* **133**, 248-281. doi:10.1098/rspb.1946.0012

Lomet, D., Cognié, J., Chesneau, D., Dubois, E., Hazlerigg, D. and Dardente, H. (2018). The impact of thyroid hormone in seasonal breeding has a restricted transcriptional signature. *Cell. Mol. Life Sci.* **75**, 905-919. doi:10.1007/s00018-017-2667-x

Milesi, S., Simonneaux, V. and Klosen, P. (2017). Downregulation of Deiodinase 3 is the earliest event in photoperiodic and photorefractory activation of the gonadotropic axis in seasonal hamsters. *Sci. Rep.* **7**, 17739. doi:10.1038/s41598-017-17920-y

Morgan, P. J., Barrett, P., Howell, H. E. and Helliwell, R. (1994). Melatonin receptors: localization, molecular pharmacology and physiological significance. *Neurochem. Int.* **24**, 101-146. doi:10.1016/0197-0186(94)90100-7

Murphy, M., Jethwa, P. H., Warner, A., Barrett, P., Nilaweera, K. N., Brameld, J. M. and Ebling, F. J. P. (2012). Effects of manipulating hypothalamic triiodothyronine concentrations on seasonal body weight and torpor cycles in Siberian hamsters. *Endocrinology* **153**, 101-112. doi:10.1210/en.2011-1249

Nakane, Y. and Yoshimura, T. (2014). Universality and diversity in the signal transduction pathway that regulates seasonal reproduction in vertebrates. *Front. Neurosci.* **8**, 1-7. doi:10.3389/fnins.2014.00115

Ono, H., Hoshino, Y., Yasuo, S., Watanabe, M., Nakane, Y., Murai, A., Ebihara, S., Korf, H.-W. and Yoshimura, T. (2008). Involvement of thyrotropin in photoperiodic signal transduction in mice. *Proc. Natl. Acad. Sci. USA* **105**, 18238-18242. doi:10.1073/pnas.0808952105

Petri, I., Diedrich, V., Wilson, D., Fernández-Calleja, J., Herwig, A., Steinlechner, S. and Barrett, P. (2016). Orchestration of gene expression across the seasons: hypothalamic gene expression in natural photoperiod throughout the year in the Siberian hamster. *Sci. Rep.* **6**, 29689. doi:10.1038/srep29689

Rasri-Klosen, K., Simonneaux, V. and Klosen, P. (2017). Differential response patterns of kisspeptin and RFamide-related peptide to photoperiod and sex steroid feedback in the Djungarian hamster (*Phodopus sungorus*). *J. Neuroendocrinol.* **29**, e12529. doi:10.1111/jne.12529

Revel, F. G., Saboureau, M., Masson-Pévet, M., Pévet, P., Mikkelsen, J. D. and Simonneaux, V. (2006a). Kisspeptin mediates the photoperiodic control of reproduction in hamsters. *Curr. Biol.* **16**, 1730-1735. doi:10.1016/j.cub.2006.07.025

Revel, F. G., Saboureau, M., Pévet, P., Mikkelsen, J. D. and Simonneaux, V. (2006b). Melatonin regulates type 2 deiodinase gene expression in the Syrian hamster. *Endocrinology* **147**, 4680-4687. doi:10.1210/en.2006-0606

Revel, F. G., Saboureau, M., Pévet, P., Simonneaux, V. and Mikkelsen, J. D. (2008). RFamide-related peptide gene is a melatonin-driven photoperiodic gene. *Endocrinology* **149**, 902-912. doi:10.1210/en.2007-0848

Ribelayga, C., Gauer, F., Calgari, C., Pévet, P. and Simonneaux, V. (1999). Photoneural regulation of rat pineal hydroxyindole-O-methyltransferase (HIOMT) messenger ribonucleic acid expression: an analysis of its complex relationship with HIOMT activity. *Endocrinology* **140**, 1375-1384. doi:10.1210/endo.140.3.6552

Sáenz de Miera, C. (2019). Maternal photoperiodic programming enlightens the internal regulation of thyroid-hormone deiodinases in tanycytes. *J. Neuroendocrinol.* **31**, e12679. doi:10.1111/jne.12679

Sáenz de Miera, C., Monecke, S., Bartzen-Sprauer, J., Laran-Chich, M.-P., Pévet, P., Hazlerigg, D. G. and Simonneaux, V. (2014). A circannual clock drives expression of genes central for seasonal reproduction. *Curr. Biol.* **24**, 1500-1506. doi:10.1016/j.cub.2014.05.024

Sáenz de Miera, C., Bothorel, B., Jaeger, C., Simonneaux, V. and Hazlerigg, D. G. (2017). Maternal photoperiod programs hypothalamic thyroid status via the fetal pituitary gland. *Proc. Natl. Acad. Sci. USA* **114**, 8408-8413. doi:10.1073/pnas.1702943114

Simonneaux, V. (2018). A Kiss to drive rhythms in reproduction. *Eur. J. Neurosci.* **51**, 1-22. doi:10.1111/ejn.14287

Smith, J. T., Dungan, H. M., Stoll, E. A., Gottsch, M. L., Braun, R. E., Eacker, S. M., Clifton, D. K. and Steiner, R. A. (2005). Differential regulation of KiSS-1 mRNA expression by sex steroids in the brain of the male mouse. *Endocrinology* **146**, 2976-2984. doi:10.1210/en.2005-0323

Smith, J. T., Coolen, L. M., Kriegsfeld, L. J., Sari, I. P., Jaafarzadehshirazi, M. R., Maltby, M., Bateman, K., Goodman, R. L., Tilbrook, A. J., Ubuka, T. et al. (2008). Variation in kisspeptin and RFamide-related peptide (RFRP) expression and terminal connections to gonadotropin-releasing hormone neurons in the brain: a novel medium for seasonal breeding in the sheep. *Endocrinology* **149**, 5770-5782. doi:10.1210/en.2008-0581

Stetson, M. H., Elliott, J. A. and Goldman, B. D. (1986). Maternal transfer of photoperiodic information influences the photoperiodic response of prepubertal Djungarian hamsters (*Phodopus sungorus sungorus*). *Biol. Reprod.* **34**, 664-669. doi:10.1095/biolreprod34.4.664

Ubuka, T., Inoue, K., Fukuda, Y., Mizuno, T., Ukena, K., Kriegsfeld, L. J. and Tsutsui, K. (2012). Identification, expression, and physiological functions of Siberian hamster gonadotropin-inhibitory hormone. *Endocrinology* **153**, 373-385. doi:10.1210/en.2011-1110

Vivien-Roels, B., Malan, A., Rettori, M.-C., Delagrange, P., Jeanniot, J.-P. and Pévet, P. (1998). Daily variations in pineal melatonin concentrations in inbred and outbred mice. *J. Biol. Rhythms* **13**, 403-409. doi:10.1177/074873098129000228

von Gall, C., Lewy, A., Schomerus, C., Vivien-Roels, B., Pevét, P. and Korf, H.-W. (2000). Transcription factor dynamics and neuroendocrine signalling in the mouse pineal gland: a comparative analysis of melatonin-deficient C57BL mice and melatonin-proficient C3H mice. *Eur. J. Neurosci.* **12**, 964-972. doi:10.1046/j.1460-9568.2000.00990.x

Weaver, D. R. and Reppert, S. M. (1986). Maternal melatonin communicates daylength to the fetus in Djungarian hamsters. *Endocrinology* **119**, 2861-2863. doi:10.1210/endo-119-6-2861

Weaver, D. R., Rivkees, S. A. and Reppert, S. M. (1989). Localization and characterization of melatonin receptors in rodent brain by *in vitro* autoradiography. *J. Neurosci.* **9**, 2581-2590. doi:10.1523/JNEUROSCI.09-07-02581.1989

Williams, L. M., Morgan, P. J., Hastings, M. H., Lawson, W., Davidson, G. and Howell, H. E. (1989). Melatonin receptor sites in the Syrian hamster brain and pituitary. Localization and characterization using [125I] Iodomelatonin. *J. Neuroendocrinol.* **1**, 315-320. doi:10.1111/j.1365-2826.1989.tb00122.x

Wittkowski, W., Bergmann, M., Hoffmann, K. and Pera, F. (1988). Photoperiod-dependent changes in TSH-like immunoreactivity of cells in the hypophysial pars tuberalis of the Djungarian hamster, *Phodopus sungorus*. *Cell Tissue Res.* **251**, 183-187. doi:10.1007/BF00215463

Yasuo, S., Yoshimura, T., Ebihara, S. and Korf, H.-W. (2009). Melatonin transmits photoperiodic signals through the MT1 melatonin receptor. *J. Neurosci.* **29**, 2885-2889. doi:10.1523/JNEUROSCI.0145-09.2009